❏   3505

An automated transmitter positioning system for misalignment compensation of capacitive-coupled electric vehicles

**Md. Nazrul Islam Siddique[1,2], Nadim Ahmed[1], Saad Mohammad Abdullah[1],
Md. Ziaur Rahman Khan[2]**

[1]Department of Electrical and Electronic Engineering, Islamic University of Technology, Gazipur, Bangladesh
[2]Department of Electrical and Electronic Engineering, Bangladesh University of Engineering and Technology, Dhaka, Bangladesh

Article Info	ABSTRACT
	Misalignments are one of the most unfavorable aspects of the capacitive power transfer (CPT) system, which is inevitable in most of the applications. Misalignments affect the overall resonances in the circuit and decrease the power transfer capability and efficiency. In this paper, an automated electro-mechanical transmitter positioning system is proposed for capacitive wireless charging to withstand both axial and rotational misalignments. The system can align the transmitter based on an adaptive algorithm, with respect to the position of the receiver to mitigate the misalignments. The overall system is designed using SolidWorks and the algorithm is verified using Processing. Then, a hardware prototype is constructed in the laboratory. The accuracy of the proposed system is calculated and compared with the simulation results. The system can achieve an accuracy of 99.5%, in case of axial misalignment and an average accuracy of 98.6%, in case of both axial and rotational misalignments, which validate the simulation results.

Corresponding Author:

Md. Nazrul Islam Siddique
Department of Electrical and Electronic Engineering, Islamic University of Technology
Board Bazar, Gazipur, Dhaka-1704, Bangladesh
Email: nazruleee@iut-dhaka.edu

1. INTRODUCTION

Over the years, fossil fuels have been the primary source of energy used in transportation. Although the demand for fossil fuel is ever so increasing, one of the major drawbacks of the continuous usage of fossil fuels is the depletion of fossil fuel reserves in the world. Moreover, burning fossil fuels to generate energy results in the emission of pollutants such as carbon dioxide (CO_2) and other greenhouse gases, which is a root cause for air pollution. According to a survey in 2017, 28.9% of the total greenhouse gas emissions in the US was resulted from the transportation sector, and it was 27% in the EU. The electric vehicle (EV) can play a huge role here to achieve environment-friendly transportation. Plug-in electric vehicles (PEV) have been proposed as an eco-friendly means of transportation. However, this technology has not gained much attraction at the consumer level due to some drawbacks related to the energy storage device such as the cost, size, and weight of the battery along with the slower charging time and low energy density [1]. Extensive research is going on in the last few decades on the development of wireless power transfer (WPT) technology-enabled electric vehicle charging to reduce these limitations. The basic advantage of WPT technology is the reduction of charging hazards and the drawbacks related to wired chargers. Other than that, several studies are being conducted to implement the WPT technology in such a way that the vehicle on board battery size could be reduced. The reduction in battery size eventually results in lower cost, reduced battery weight, and faster charging [2]. The wireless charging scheme can reduce the battery size to 27-44%

of a PEV battery [3]. Furthermore, compared to PEV, 0.3% less energy consumption and 0.5% of less greenhouse gas emissions can be achieved through the wireless charging system.

Two techniques-inductive power transfer (IPT) [4], [5] and capacitive power transfer (CPT) [6], [7] have been used effectively for WPT applications in recent decades. The development of IPT system has been widely investigated and it is used in numerous applications such as sensor networks [8], biomedical devices [9], integrated circuits (IC) [10] and electric vehicles [11]. However, IPT has some setbacks such as electromagnetic radiation, which is pernicious to human health and it produces eddy current losses around metal objects due to the high-frequency magnetic fields which limit its applications, for example, electric vehicle charging [12], [13]. CPT can be an attractive alternative to IPT in these kinds of applications [14]. CPT system utilizes high-frequency electric fields as the means of power transfer [15]. CPT system has several advantages, including less heating, less eddy current losses, the design flexibility of the coupling structure, and better misalignment tolerance compared to IPT [16].

Although the CPT system provides better misalignment performance compared to IPT system, the misalignments between transmitter and receiver plates still remain a concern as any misalignment causes the coupling capacitance to decrease and affects the resonances in the CPT system which altogether degrades the power efficiency and limits the amount of power transferred wirelessly. For CPT systems, researchers have used different compensation networks through combination of different inductors (L) and capacitors (C). In study [17], a double-sided LCLC compensated CPT system was proposed and for a misalignment of 300 mm, it was observed that the output power decreases by 12.5% of the well-aligned case. In study [18], a four-plate LCL-compensated capacitive coupler design was proposed and it was shown that for a 300 mm misalignment along X-axis, the system power dropped approximately 56.4% of that of the completely aligned case. In case of rotational misalignment, the power ripple was found to be within ±5% of the nominal power. For a double-sided LC compensated CPT system [19], it was presented that for a misalignment of 200 mm, the mutual capacitance between the transmitter and receiver decreases about 54.2% of the well-aligned case. A two-plate CPT system proposed in [20]. In this study, it was shown that for a misalignment of 80 mm, the output power dropped to 46% of the well-aligned case, whereas, the power level reduced to 12% of the well-aligned case when the misalignment was increased to 150 mm. The misalignments effect was also investigated in [21] and was noticed that vertically arranged capacitive coupler structure is more sensitive to misalignments compared to horizontal system. An adaptive robotic arm was proposed for the IPT system so that it can place the receiving coil on top of the transmitter to get the well alignment between the transmitting and receiving coils to get the maximum power transfer efficiency [22]. However, the arm was placed on the vehicle chassis which added complicacy to the vehicle design and increased the vehicle weight as well. Dai and Ludois [23] have proposed CPT charging through a conformal bumper which reduced the air gap, minimized the misalignments and confined the field. Nevertheless, there is a direct contact between the transmitter and the receiver, so it cannot be called as a WPT system.

In this paper, an automated transmitter positioning system is proposed for a capacitive coupled electric vehicle considering the disadvantageous aspects of misalignment. The transmitter moves in order to align itself with the receiver in case of any kind of axial and rotational misalignments in the proposed system. The complete alignment of the transmitter and the receiver is expected to facilitate the output power level and efficiency.

The paper is organized. The section 2 gives a brief overview of the system. In the section 3, proposed transmitter positioning system is presented. Hardware implementation of the system is outlined in section 4. The section 5 delineated the experimental results and discussion. The conclusions are drawn in the final section.

2. PLATE STRUCTURE AND CIRCUIT MODEL
2.1. Plate structure

The structure and dimensions of a four plate compact capacitive coupler are shown in Figure 1(a). The structure consists of four metal plates, P_1 to P_4. Plates P_1 and P_2 are vertically embedded on the ground in the same horizontal plane as a transmitter. Plates P_3 and P_4 are also vertically arranged and installed on the vehicle side as a receiver. The size of plates P_1 and P_3 are larger than P_2 and P_4. All the plate shapes are chosen to be square. In this design, the length of P_1 and P_3 is l_1 and l_2 is the length of P_2 and P_4. The distance between the plates on the same side is defined as d_c. d is the air gap distance between P_2 and P_4. There is coupling capacitance between each pair of plates as illustrated in Figure 1(b). As the distance d is much larger than dc in vehicle charging applications, C_{12} and C_{34} will be larger than C_{13} and C_{24}. Due to the edge effect of P_1-P_4 and P_2-P_3, there are cross-couplings capacitance C_{14} and C_{23}. The equivalent self-capacitance at the primary side is defined as C_1 and the secondary side is defined as C_2, and the mutual capacitance is defined as C_M. The relationship between these parameters is shown in (1).
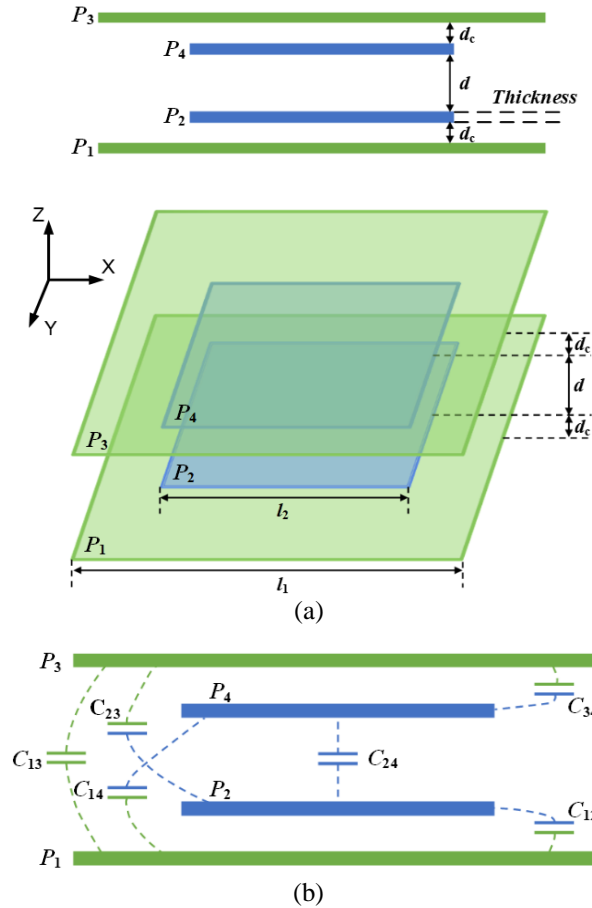
Figure 1. Design of CPT system (a) structure and dimensions of the plates and (b) coupling capacitors between the plates [18]

$$\begin{cases} C_1 = C_{12} + \dfrac{(C_{13} + C_{14}) \cdot (C_{23} + C_{24})}{C_{13} + C_{14} + C_{23} + C_{24}} \\ C_2 = C_{34} + \dfrac{(C_{13} + C_{23}) \cdot (C_{14} + C_{24})}{C_{13} + C_{14} + C_{23} + C_{24}} \\ C_M = \dfrac{C_{13}C_{24} - C_{14}C_{23}}{C_{13} + C_{14} + C_{23} + C_{24}} \end{cases} \tag{1}$$

2.2. Compensation network

A full-bridge inverter based double sided LCL compensation circuit [24] is shown in Figure 2. A direct current (DC) voltage source, V_{in} is used at the primary side and a full-bridge metal oxide semiconductor field effect transistor (MOSFET) inverter converts this dc voltage to alternating current (AC) in order to provide excitation to the resonant circuit. At the secondary side, a full-bridge uncontrolled diode rectifier is used to provide current to the load, V_{out} which can represent the battery in the electric vehicle. The output power, pout can be written as (2):

$$P_{out} = |V_1||I_1| = w C_M \cdot \frac{C_{f1} \cdot C_{f2}}{C_1 C_2} \cdot |V_1||V_2| \tag{2}$$

Considering the input dc voltage, V_{in} and the battery voltage, V_{out} in Figure 2, (2) can be rewritten as (3):

$$P_{out} = |V_1||I_1| = w C_M \cdot \frac{C_{f1} \cdot C_{f2}}{C_1 C_2} \cdot \frac{2\sqrt{2}V_{in}}{\pi} \cdot \frac{2\sqrt{2}V_{out}}{\pi} \tag{3}$$

The equation (3) shows that the output power is approximately proportional to the mutual capacitance, C_M. So, C_M should be maximized to get the maximum power transfer. There are other compensation topologies such as LCLC [17], CLLC [25], LCLL [26] and the power and mutual capacitance relationship are same like LCL.
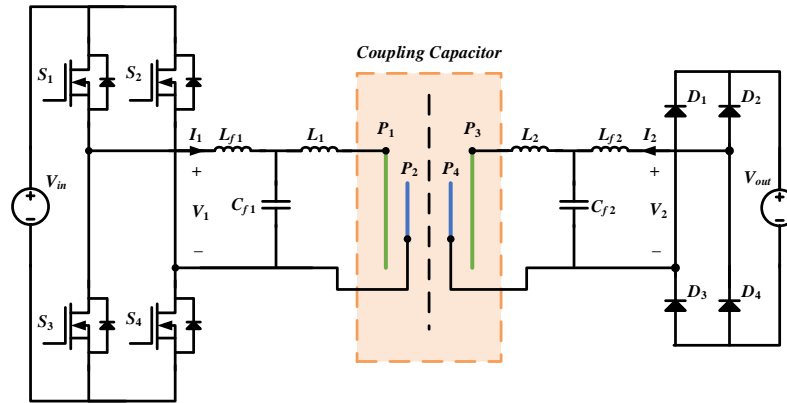
Figure 2. Double-sided LCL compensated circuit topology

2.3. Effect of misalignments on mutual capacitance

There are two types of misalignments considered in this paper-axial misalignment (X and Y axis misalignment) and rotational or angular misalignment. Ansoft Maxwell is used to determine the mutual capacitance, C_M for different misalignment conditions. For the simulation; l_1=440 mm, l_2=310 mm, d_c=10 mm and d=150 mm are considered. These dimensions are considered with respect to the dimensions of the hardware design of the positioning system described later in section 4.

It is seen from Figures 3(a) and 3(b) that, if there is any misalignment along X-axis and Y-axis respectively, then in both cases the mutual capacitance, C_M between the transmitter and the receiver decreases, which will cause deterioration of the system output power and the total efficiency. C_M is maximum when there is zero misalignment which is clearly evident from Figures 3(a) and 3(b). Thus, the goal of this research is to design an automated transmitter positioning system which will compensate positional deviation between the transmitter and the receiver in order to obtain the zero-misalignment condition.
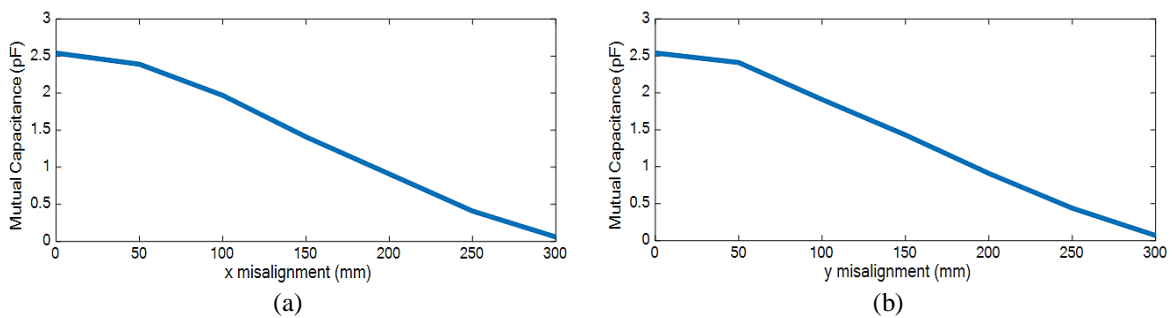

| (a) | (b) |

Figure 3. C_M at different misalignment conditions (a) X misalignment and (b) Y misalignment

3.   DESIGN OF THE AUTONOMOUS TRANSMITTER POSITIONING SYSTEM

The proposed model of the automated transmitter positioning system is designed using SolidWorks as detailed in Figure 4(a). The whole system is surrounded by an outer metal frame. Two square non-conducting plates are collectively considered as the base for the transmitter. On top of these base plates, the transmitter is mounted. One of these two base plates is static, whereas the other one can rotate around its center termed as the revolving axis. In order to detect the presence of the receiver, the rotational base is equipped with five infrared (IR) sensors as shown in Figure 4(b). The rotational base is attached to the static base through a stepper motor which controls its angular movement. The front shaft of the stepper motor is connected to the rotational base through two gears to increase the torque output as shown in Figure 5(a). For the purpose of taking the angular feedback of the rotating base, a rotary encoder is attached to the back shaft of the stepper motor by means of a belt-pulley system as shown in Figure 5(b). The static base of this cone penetration test (CPT) system is mounted on two shafts along which it can move in the Y-direction. Clamps are used to attach the shafts ends with two movable metal frames. Four linear bearings are used to couple the

static base with the shafts for the smooth movement of the transmitter which is visible from the rear-view image depicted in Figure 5(b). The movement along the Y-axis is controlled by a stepper motor and a belt-pulley mechanism within the movable frame. In order to move the base along the X-axis, this movable frame is further attached with two shafts through linear bearings. These two shafts are attached firmly with the outer frame using clamps and another stepper motor and belt-pulley mechanism are used to control the movement of the movable frames along the X-axis. Moreover, there are three limit switches attached to the system in order to signify the limits along the X, Y and revolving axis as shown in Figure 4(a). The feedback from these limit switches is used to retain the transmitter to its initial position after completing the charging of the battery. The misalignments between the transmitter and the receiver are extenuated based on the feedback from the sensors and the encoder, affixed to the rotating base depending on an algorithm discussed in the following section.
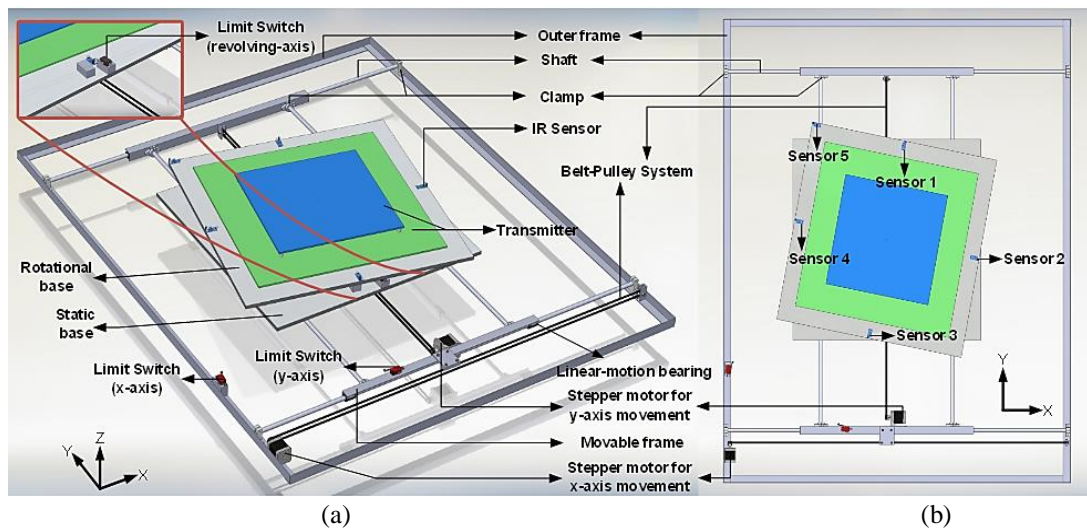

(a)   (b)

Figure 4. SolidWorks design of the proposed system (a) 3D view and (b) 2D view

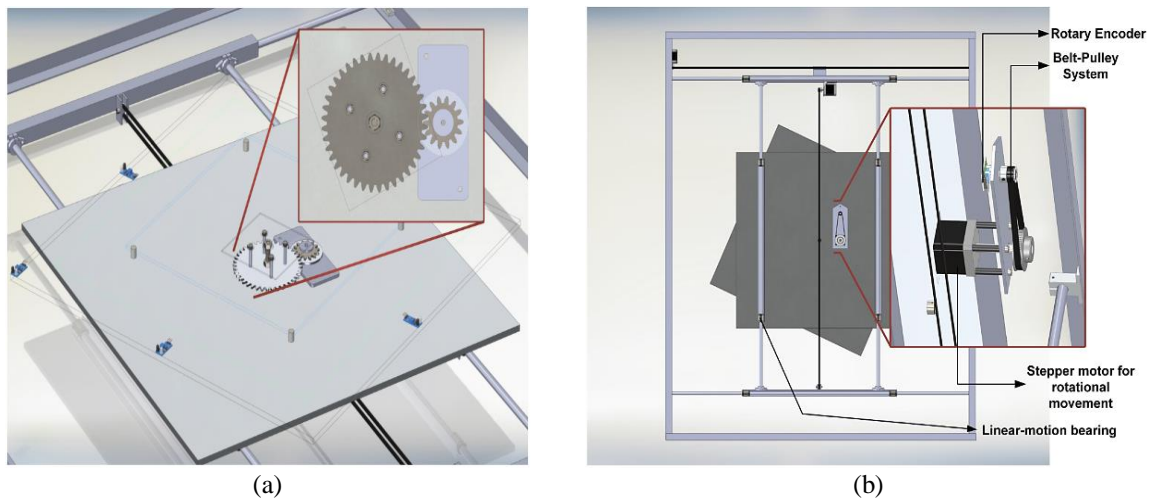(a)   (b)

Figure 5. SolidWorks design of (a) the gear mechanism associated with the rotational base and (b) connection of the rotary encoder

4.   HARDWARE SETUP
4.1. Prototype design

The whole system is presented in a block diagram as illustrated in Figure 6. A prototype of our proposed system is built in the laboratory as shown in Figure 7(a). In our design, two square plates are used as two bases having dimensions of 460×460 mm; one is static and another one is rotational. On top of the

static base, the rotational base is mounted. The transmitter plates will be mounted on top of the rotational base by means of non-conducting material. Since the power transfer is not the main focus of this research, only the alignment is; the transmitter plates were not attached in the prototype. The capability of the rotating base at the transmitting side to be aligned with the base at the receiving side was tested for different combinations of misalignment as this is the same as aligning the transmitter with the receiver. Thus, in this research the terms rotating base and transmitter are used interchangeably. The outer frame is made of stainless steel and the dimension is 1220×910 mm. Within the outer frame, an area of 910×910 mm is covered by the movable metal frames on top of which the static and rotational base at the transmitter side is attached through shafts and linear bearings. Thus, any misalignments between these areas are expected to be mitigated by this system. Two of the four shafts are connected to the outer frame with the help of clamps. Four linear bearings are used to attach the movable frames along these two shafts. The movable frames contain the remaining two shafts which are connected via clamps. Again, four linear bearings are used to mount the base plates on top of the two shafts of the movable frames. Five IR proximity sensors are placed on the rotational base in order to detect the position of the receiver. The sensors 1-4, which are responsible to mitigate axial misalignment, are placed in the middle of each side of the rotational base and sensor 5 is placed at the edge of top left corner which is responsible for mitigating the rotational misalignment as shown in Figure 4(b).

As a power source, AC supply is provided which is converted to 12 V DC using a rectifier as illustrated in Figure 6. Then, the power is supplied to the Arduino Mega 2560, which is used as a controller and the four motor drivers, A4988. The sensors and encoder are powered up by the Arduino and the feedback from these components is fed to the controller. Depending on the signal, Arduino controls the stepper motor based on the proposed algorithm. The controller unit of the prototype is shown in Figure 7(b). Only stepper motor 1 and 2 function in case of axial misalignment. Stepper motor 3 is employed to rotate the base and the base is connected to the front shaft of the motor through two gear to increase the torque output. The larger gear has 40 teeth and the smaller one has 14 teeth. Therefore, the degree rotation of revolving axis per step of stepper motor: $((14/40) \times 0.225) = 0.07875°$/step due to the eighth step setting of the driver and the gear mechanism. For rotational feedback of this axis, a rotary encoder (KY-040) has been employed, which has an accuracy of 20 pulses per revolution. To improve the accuracy, a belt-pulley system at the back shaft of the stepper motor is fixed to get encoder pulses from the motor as shown in Figure 7(c). A big pulley is connected with the motor and has 60 teeth; the smaller pulley has 20 teeth. With gear and belt-pulley setup, accuracy of the encoder: $((20/60) \times (14/40) \times 18) = 2.1°$/pulse. Hence, for every 2.1° rotation of the base, the encoder provides the rotational feedback to the controller.
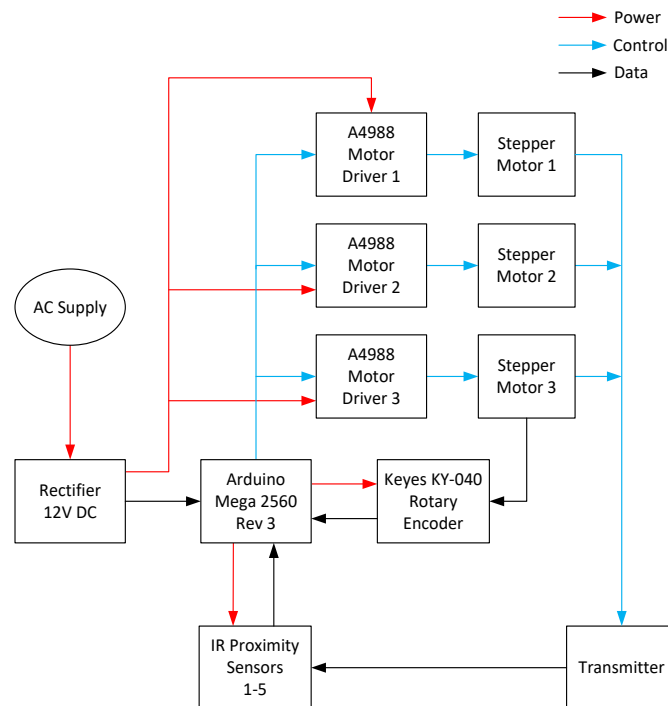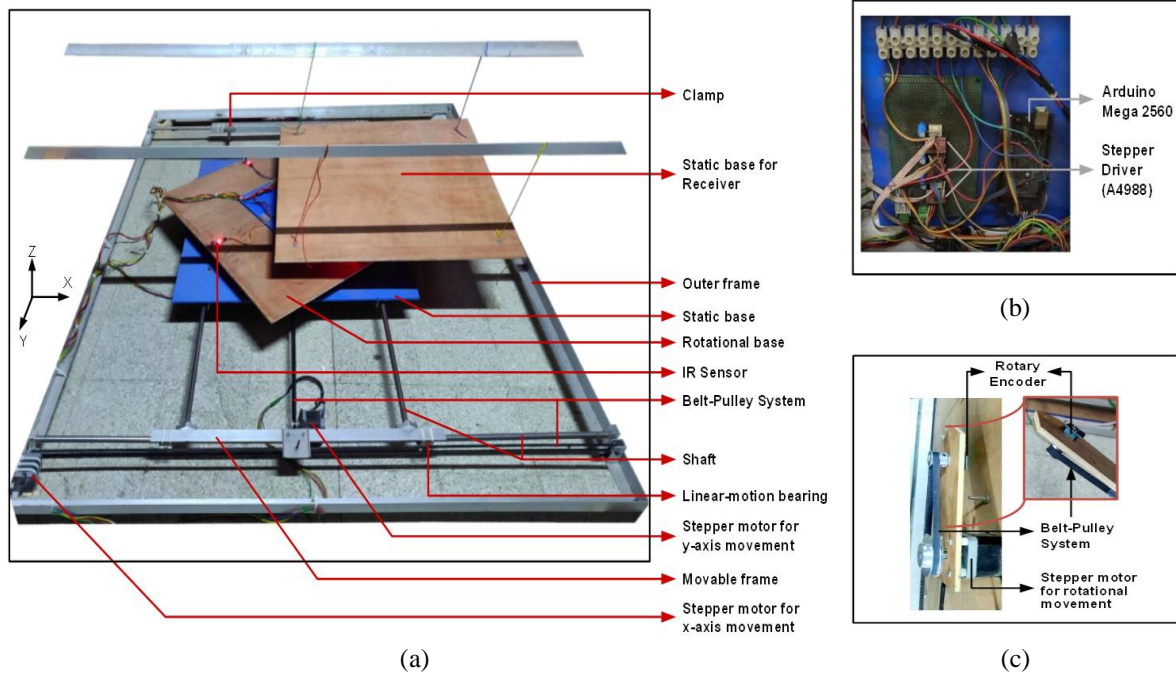

Figure 6. Block diagram of the proposed system

Figure 7. Prototype of the proposed system; (a) complete view, (b) controller unit, and (c) connection of the rotary encoder

4.2. Formulation of the algorithm

Usually, the drivers are most likely to park their vehicle using the sides of the parking bay as an alignment guide. The proposed transmitter positioning system along with the alignment guide and the vehicle parked on the proposed system are illustrated in Figure 8(a) and 8(b) respectively. Moreover, there is an IR proximity sensor placed on the ground which notifies the driver to stop the vehicle by buzzing a buzzer for a short amount of time. After getting the feedback from this sensor, the system is powered up and the algorithm is initiated. The algorithm is written in Arduino IDE and implemented on the microcontroller Arduino Mega 2560. Figure 9 illustrates the basic operation of the proposed algorithm. The algorithm functions in following the fashion:

Step 1: First, the transmitter is at its initial place which is positioned by the three limit switches. The status (1 or 0) of the sensors 1 to 4 are read.

Step 2: The transmitter moves in the XY plane with the help of the stepper motors along X and Y axis from its initial position depending on the feedback from the sensor (s) as indicated in Table 1.

Step 3: When all the four sensors detect the receiving plate, the status of sensor 5 is read.

Step 4: If the sensor 5 does not indicate any reading, that means there is rotational misalignment, and the transmitter is not completely aligned with the receiver. An iterative process, described as followed: i) transmitter rotates at an angle of 0.07875° (step angle of the motor) in the clockwise direction, ii) the status of sensors 1 to 4 are checked again after every 2.1° (resolution of the encoder). If any of these sensors is out of the bound, the transmitter moves accordingly as indicated in Table 1 in the XY plane until all the four sensors show the reading, and iii) the process continues until all five sensors provide the feedback to the controller and the alignment between the transmitter and receiver is achieved.

After completing the charging of the battery, the vehicle is out of the parking bay. The proximity sensor as shown in Figure 8 updates the controller about the status of the vehicle. Then, the transmitter is brought back to its initial position so that the system is ready to initialize another charging process. In order to assure that, first, the transmitter is rotated in anti-clockwise direction until the limit switch along the revolving axis gets a reading. After that, the transmitter is moved along the Y axis towards the limit switch as shown in Figures 4(a) and 4(b). When the transmitter touches this limit switch, the movement of the transmitter along X axis towards the limit switch is initiated. Upon receiving the feedback from these three limit switches, the initial position of the transmitter is obtained.
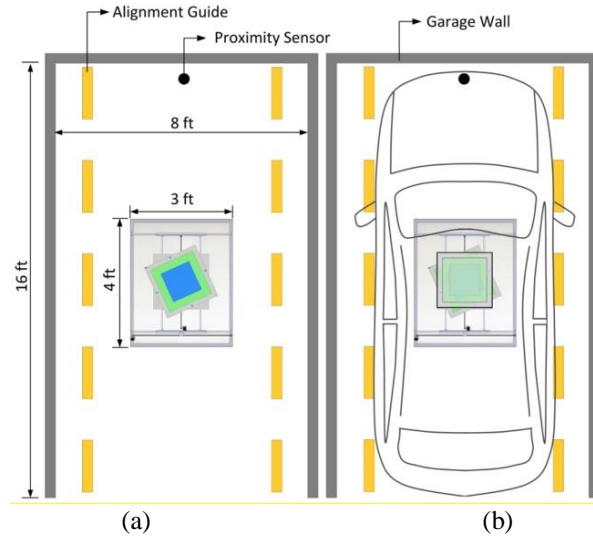
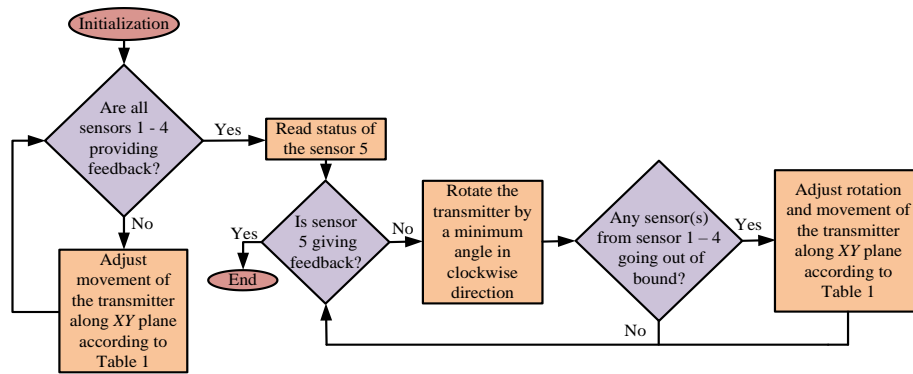Figure 8. Parking bay: (a) transmitter dimensions along with alignment guide, and (b) vehicle parked inside

Figure 9. Flowchart of the proposed algorithm

Table 1. Rotation of motors based on the feedback from the sensors

Feedback from sensors				Rotation of motors		Transmitter movement	
Sensor 4	Sensor 3	Sensor 2	Sensor 1	Along X axis	Along Y axis	Along X axis	Along Y axis
0	0	0	0	Clockwise	Clockwise	Positive	Positive
0	0	0	1	x	Clockwise	x	Positive
0	0	1	0	Clockwise	x	Positive	x
0	0	1	1	Clockwise	Clockwise	Positive	Positive
0	1	0	0	x	Anti-clockwise	x	Negative
0	1	1	0	Clockwise	Anti-clockwise	Positive	Negative
0	1	1	1	Clockwise	x	Positive	x
1	0	0	0	Anti-clockwise	x	Negative	x
1	0	0	1	Anti-clockwise	Clockwise	Negative	Positive
1	0	1	1	Clockwise	x	Positive	x
1	1	0	0	Anti-clockwise	Anti-clockwise	Negative	Negative
1	1	0	1	Anti-clockwise	x	Negative	x
1	1	1	0	x	Anti-clockwise	x	Negative
1	1	1	1	x	x	x	x

*The transmitter movement in the right-hand side and in the upper direction is considered positive and otherwise, negative. x indicates no rotation of the motors.

4.3. Validation of the algorithm

Our proposed algorithm is validated using processing. The algorithm is tested under different possible misalignment cases of the receiver with respect to the transmitter. The algorithm works perfectly fine for every case of misalignments. Two of these cases are illustrated in Figures 10(a) and 10(b).
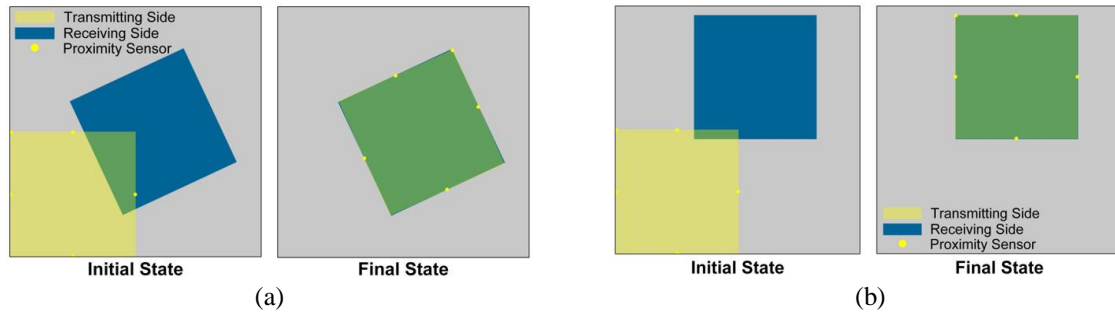
Figure 10. Validation through processing (a) axial and rotational misalignments and (b) only axial misalignment

5. RESULTS AND DISCUSSION

The accuracy of the proposed system is experimentally tested under the same misalignment cases, considered in the software validation and a comparison between simulation results and practical findings are listed in Table 2. The accuracy is calculated based on the overlapping area between the plates. Moreover, the time required to compensate for misalignments in the hardware setup is also tabulated. It is observed that the system can achieve an accuracy of more than 99% for the axial misalignment (X and Y) and about 98% for both axial and rotational misalignments which is quite consistent with the simulation results. Increasing overlapping area means increasing the mutual capacitance which will heighten the output power. It can be seen from Figure 11 that without the proposed transmitter positioning system the mutual capacitance drops with increasing misalignments but with the proposed positioning system, the system can maintain a constant mutual capacitance for about 450 mm which is the maximum tolerance limit of the proposed system.

Table 2. Experimental results

Misalignments			Simulation accuracy (%)	Experimental Accuracy (%)	Compensation time (s)	Misalignments			Simulation accuracy (%)	Experimental Accuracy (%)	Compensation time (s)
Axial misalignments (mm)		Angular misalignments (°)				Axial misalignments (mm)		Angular misalignments (°)			
X axis	Y axis					X axis	Y axis				
200	100	0	99.67	99.04	6.77	350	400	15	99.21	98.93	35.92
350	400	0	99.67	99.02	13.5	200	100	20	99.28	98.67	31.21
200	100	5	99.31	98.66	26.96	350	400	20	99.22	98.52	37.29
350	400	5	99.31	98.65	33.69	200	100	25	99.43	98.8	32.76
200	100	10	99.38	98.64	28.41	350	400	25	99.42	98.81	38.57
350	400	10	99.46	98.7	34.71	200	100	30	99.18	98.12	33.98
200	100	15	99.56	98.97	29.5	350	400	30	99.34	97.79	39.74

However, there are some limitations to the proposed system. It is observed that the accuracy is consistent for only the axial misalignment but when the rotational misalignments are accumulated in the system, the accuracy is inconsistent. This is due to the possible mismatch between the encoder resolution and the step angle of the motor associated with rotating the transmitter. Due to the proposed algorithm, the system checks for any possible axial misalignments due to the angular movement after every 2.1°. Then, the system adjusts the transmitter to mitigate the axial misalignment and proceeds to mitigating the rotational misalignment afterward with aid from the motor and the process continues until all the five sensors get the reading. For example, rotational misalignments of 5°, the system adjusts the transmitter two times (every 2.1°) after the rotation of the transmitter to mitigate the axial misalignments resulting in the change of rotational angle and finally mitigate both misalignments. Thus, due to this adjustment and the step angle of the motor, the rotation of the transmitter could be greater or smaller than the actual rotational misalignments. Hence, accuracy varies randomly depending on the initial axial and rotational misalignments. Therefore, the encoder and the motor for the rotating axis, having the same resolution could be adopted to get the best accuracy of the proposed system. Moreover, some errors are amassed due to the sensor position on the base as sometimes sensors located under the receiving plate provide feedback when the receiving plates are in close proximity of the sensors (2-3 cm) not exactly on top of it resulting in some non-overlapping area between the plates. Also, due to the inertia effect, the transmitter tends to move for a fraction of time after terminating the compensation process resulting in some change in the overlapping area. Also, the stepper

motor employed for rotating the transmitter is sometimes unable to produce enough torque to provide the precise angle rotation. Thus, a stepper motor having high torque such as Nema 23 could be utilized to overcome this limitation. Moreover, the shafts that are used for the X and Y axis are not stiff enough and vibrate during the operation. Hence, shafts with a higher diameter like 25 mm could be utilized.
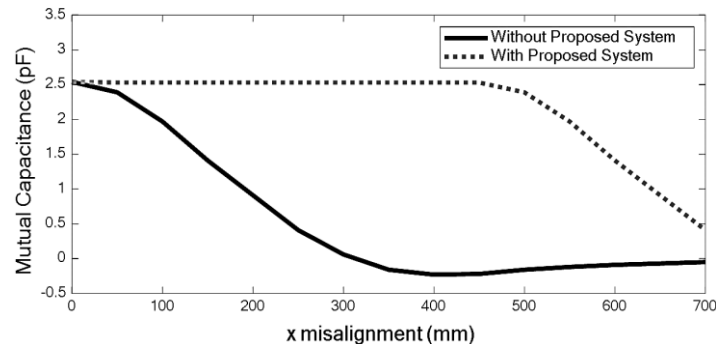

Figure 11. Mutual capacitance with and without proposed system

6. CONCLUSION

In this paper, the main focus was to develop an adaptive transmitter positioning system for a capacitive power transfer (CPT) system to mitigate the disadvantages associated with the misalignments between the transmitter and receiver plates of the electric vehicles. In order to operate the adaptive system, an algorithm was developed in this study which could compensate both axial and angular misalignments between the transmitter and the receiver irrespective of the system parameters in the system. The physical design of the proposed system was first developed in SolidWorks and later on, a hardware prototype was constructed based on the design. The accuracy of the proposed system was validated through a series of software and hardware tests. The software tests were carried out using Processing where an accuracy of 99.39% was obtained on an average, considering different cases of axial and angular misalignments. On the contrary, for the same set of misalignments, an average accuracy of 98.6% was obtained in experimental setup. In light of the software and hardware validations, the proposed system can be considered as a prospective solution to the misalignments problems associated with the CPT system for static wireless vehicle charging applications since the system is simple and efficient. In future work, the transmitter will be mounted on the rotating base and the power transfer stability in case of misalignments will be observed.

REFERENCES

[1] D. M. Vilathgamuwa and J. P. K. Sampath, "Wireless power transfer (WPT) for electric vehicles (EVs)-present and future trends," in *Power Systems*, vol. 91, Springer, Singapore, 2015, pp. 33–60.

[2] L. Chen, G. R. Nagendra, J. T. Boys, and G. A. Covic, "Double-coupled systems for IPT roadway applications," *IEEE Journal of Emerging and Selected Topics in Power Electronics*, vol. 3, no. 1, pp. 37–49, Mar. 2015, doi: 10.1109/JESTPE.2014.2325943.

[3] Z. Bi, L. Song, R. De Kleine, C. C. Mi, and G. A. Keoleian, "Plug-in vs. wireless charging: Life cycle energy and greenhouse gas emissions for an electric bus system," *Applied Energy*, vol. 146, pp. 11–19, May 2015, doi: 10.1016/j.apenergy.2015.02.031.

[4] J. H. Kim *et al.*, "Development of 1-MW inductive power transfer system for a high-speed train," *IEEE Transactions on Industrial Electronics*, vol. 62, no. 10, pp. 6242–6250, Oct. 2015, doi: 10.1109/TIE.2015.2417122.

[5] C. Zheng, H. Ma, J.-S. Lai, and L. Zhang, "Design considerations to reduce gap variation and misalignment effects for the inductive power transfer system," *IEEE Transactions on Power Electronics*, vol. 30, no. 11, pp. 6108–6119, Nov. 2015, doi: 10.1109/TPEL.2015.2424893.

[6] D. C. Ludois, M. J. Erickson, and J. K. Reed, "Aerodynamic fluid bearings for translational and rotating capacitors in noncontact capacitive power transfer systems," *IEEE Transactions on Industry Applications*, vol. 50, no. 2, pp. 1025–1033, Mar. 2014, doi: 10.1109/TIA.2013.2273484.

[7] J. Dai and D. C. Ludois, "A survey of wireless power transfer and a critical comparison of inductive and capacitive coupling for small gap applications," *IEEE Transactions on Power Electronics*, vol. 30, no. 11, pp. 6017–6029, Nov. 2015, doi: 10.1109/TPEL.2015.2415253.

[8] Liguang Xie, Yi Shi, Y. T. Hou, and A. Lou, "Wireless power transfer and applications to sensor networks," *IEEE Wireless Communications*, vol. 20, no. 4, pp. 140–145, Aug. 2013, doi: 10.1109/MWC.2013.6590061.

[9] S. Stoecklin, A. Yousaf, T. Volk, and L. Reindl, "Efficient wireless powering of biomedical sensor systems for multichannel brain implants," *IEEE Transactions on Instrumentation and Measurement*, vol. 65, no. 4, pp. 754–764, Apr. 2016, doi: 10.1109/TIM.2015.2482278.

[10] N.-C. Kuo, B. Zhao, and A. M. Niknejad, "Inductive wireless power transfer and uplink design for a CMOS tag with 0.01 mm 2 coil size," *IEEE Microwave and Wireless Components Letters*, vol. 26, no. 10, pp. 852–854, Oct. 2016, doi: 10.1109/LMWC.2016.2605440.

[11] M. Kim, H. Kim, D. Kim, Y. Jeong, H.-H. Park, and S. Ahn, "A three-phase wireless-power-transfer system for online electric vehicles with reduction of leakage magnetic fields," *IEEE Transactions on Microwave Theory and Techniques*, vol. 63, no. 11, pp. 3806–3813, Nov. 2015, doi: 10.1109/TMTT.2015.2479627.

[12] S. A. Mirbozorgi, H. Bahrami, M. Sawan, and B. Gosselin, "A smart cage with uniform wireless power distribution in 3D for enabling long-term experiments with freely moving animals," *IEEE Transactions on Biomedical Circuits and Systems*, vol. 10, no. 2, pp. 424–434, Apr. 2016, doi: 10.1109/TBCAS.2015.2414276.

[13] C. Xiao, K. Wei, D. Cheng, and Y. Liu, "Wireless charging system considering eddy current in cardiac pacemaker shell: theoretical modeling, experiments, and safety simulations," *IEEE Transactions on Industrial Electronics*, vol. 64, no. 5, pp. 3978–3988, May 2017, doi: 10.1109/TIE.2016.2645142.

[14] Y.-G. Su, S.-Y. Xie, A. P. Hu, C.-S. Tang, W. Zhou, and L. Huang, "Capacitive power transfer system with a mixed-resonant topology for constant-current multiple-pickup applications," *IEEE Transactions on Power Electronics*, vol. 32, no. 11, pp. 8778–8786, Nov. 2017, doi: 10.1109/TPEL.2016.2640314.

[15] D. Shmilovitz, S. Ozeri, and M. M. Ehsani, "A resonant LED driver with capacitive power transfer," in *2014 IEEE Applied Power Electronics Conference and Exposition-APEC 2014*, Mar. 2014, pp. 1384–1387, doi: 10.1109/APEC.2014.6803487.

[16] T. Komaru and H. Akita, "Positional characteristics of capacitive power transfer as a resonance coupling system," in *2013 IEEE Wireless Power Transfer (WPT)*, May 2013, pp. 218–221, doi: 10.1109/WPT.2013.6556922.

[17] F. Lu, H. Zhang, H. Hofmann, and C. Mi, "A double-sided LCLC-compensated capacitive power transfer system for electric vehicle charging," *IEEE Transactions on Power Electronics*, vol. 30, no. 11, pp. 6011–6014, Nov. 2015, doi: 10.1109/TPEL.2015.2446891.

[18] H. Zhang, F. Lu, H. Hofmann, W. Liu, and C. C. Mi, "A four-plate compact capacitive coupler design and LCL-compensated topology for capacitive power transfer in electric vehicle charging application," *IEEE Transactions on Power Electronics*, vol. 31, no. 12, pp. 8541–8551, Dec. 2016, doi: 10.1109/TPEL.2016.2520963.

[19] H. Zhang, F. Lu, H. Hofmann, and C. Mi, "A loosely coupled capacitive power transfer system with LC compensation circuit topology," in *2016 IEEE Energy Conversion Congress and Exposition (ECCE)*, Sep. 2016, pp. 1–5, doi: 10.1109/ECCE.2016.7854702.

[20] F. Lu, H. Zhang, and C. Mi, "A two-plate capacitive wireless power transfer system for electric vehicle charging applications," *IEEE Transactions on Power Electronics*, vol. 33, no. 2, pp. 964–969, Feb. 2018, doi: 10.1109/TPEL.2017.2735365.

[21] M. Al-Saadi, E. A. Hussien, S. Ahmed, and A. Craciunescu, "Comparative study of compensation circuit topologies in 6.6kW capacitive power transfer system," in *2019 11th International Symposium on Advanced Topics in Electrical Engineering (ATEE)*, Mar. 2019, pp. 1–6, doi: 10.1109/ATEE.2019.8725012.

[22] M. R. Barzegaran, H. Zargarzadeh, and O. A. Mohammed, "Wireless power transfer for electric vehicle using an adaptive robot," *IEEE Transactions on Magnetics*, vol. 53, no. 6, pp. 1–4, Jun. 2017, doi: 10.1109/TMAG.2017.2664800.

[23] J. Dai and D. C. Ludois, "Capacitive power transfer through a conformal bumper for electric vehicle charging," *IEEE Journal of Emerging and Selected Topics in Power Electronics*, vol. 4, no. 3, pp. 1015–1025, Sep. 2016, doi: 10.1109/JESTPE.2015.2505622.

[24] H. Zhang, F. Lu, H. Hofmann, W. Liu, and C. Mi, "A large air-gap capacitive power transfer system with a 4-plate capacitive coupler structure for electric vehicle charging applications," in *2016 IEEE Applied Power Electronics Conference and Exposition (APEC)*, Mar. 2016, vol. 2016-May, pp. 1726–1730, doi: 10.1109/APEC.2016.7468100.

[25] F. Lu, H. Zhang, H. Hofmann, and C. Mi, "A CLLC-compensated high power and large air-gap capacitive power transfer system for electric vehicle charging applications," in *2016 IEEE Applied Power Electronics Conference and Exposition (APEC)*, Mar. 2016, vol. 2016-May, pp. 1721–1725, doi: 10.1109/APEC.2016.7468099.

[26] V.-B. Vu, M. Dahidah, V. Pickert, and V.-T. Phan, "An improved LCL-L compensation topology for capacitive power transfer in electric vehicle charging," *IEEE Access*, vol. 8, pp. 27757–27768, 2020, doi: 10.1109/ACCESS.2020.2971961.

BIOGRAPHIES OF AUTHORS

Md. Nazrul Islam Siddique ⓘ 🔗 SC Ⓟ is currently a Ph.D. student at the University of New South Wales, Australia. He completed his B.Sc. from Islamic University of Technology, Bangladesh and M.Sc. from Bangladesh University of Engineering and Technology, Bangladesh both in Electrical and Electronic Engineering. His research is focused on power system, renewable energy, and wireless power transfer. He can be contacted at email: nazruleee@iut-dhaka.edu.

Nadim Ahmed ⓘ 🔗 SC Ⓟ received his B.Sc. degree in Electrical and Electronic Engineering from Islamic University of Technology, Bangladesh in 2019. Currently, he is serving as a lecturer in Islamic University of Technology. His main research interests include machine learning, computer vision, autonomous vehicle technologies, embedded and FPGA-based system design. He can be contacted at email: nadimahmed@iut-dhaka.edu.

Saad Mohammad Abdullah 🆔 🔾 SC Ⓟ received his B.Sc. and M.Sc. degrees from the Department of Electrical and Electronic Engineering (EEE), Islamic University of Technology (IUT), Gazipur, Bangladesh, in 2016 and 2019, respectively. He is currently working as a faculty member in the Department of EEE, IUT. His research interests include microgrids, engineering optimization, and wireless power transfer. He can be contacted at email: saadabdullah@iut-dhaka.edu.

Md. Ziaur Rahman Khan 🆔 🔾 SC Ⓟ is a professor at the department of Electrical and Electronic Engineering in Bangladesh University of Engineering and Technology, Dhaka, Bangladesh. He obtained B.Sc. and M.Sc. degrees in Electrical and Electronic Engineering from the same institute. He completed his Ph.D. from University of Cambridge, UK in 2009. His research interests include power electronics, renewable energy systems, electronic device modeling and simulation. He has published numerous articles in reputed conferences and journals. He can be contacted at email: zrkhan@eee.buet.ac.bd.